Hindawi
Advances in Civil Engineering
Volume 2021, Article ID 6633706, 10 pages
https://doi.org/10.1155/2021/6633706

Research Article

Analysis of Corrosion-Fatigue Damage and Fracture Mechanism of In-Service Bridge Cables/Hangers

Yao Guowen,[1] **Yang Shicong**,[1] **Zhang Jinquan**,[1,2] **and Leng Yanling**[3]

[1]*State Key Laboratory of Mountain Bridge and Tunnel Engineering, Chongqing Jiaotong University, Chongqing 400067, China*
[2]*Beijing Research Institute of Highway, Ministry of Transport, Beijing 100088, China*
[3]*New Mexico State University, Las Cruces, NM 88001, USA*

Correspondence should be addressed to Yao Guowen; 379062524@qq.com

Received 9 December 2020; Revised 9 January 2021; Accepted 19 January 2021; Published 10 February 2021

Academic Editor: Claudio Mazzotti

Cables/hangers are important load-bearing components of suspension, cable-stayed, and through-arch bridges. Their reliability throughout their service life directly affects the safety of these bridges. In this study, to provide a reference for the design, maintenance, and inspection of bridge cables/hangers, their damage and failure mechanisms were theoretically analyzed using finite element analysis and corrosion-fatigue simulation tests of steel wires, based on the characteristics of the cable/hanger damage. The finite element analysis showed that a rotation of 0.00113 rad in the lower anchorage area results in a bending stress of 18.8 MPa, indicating that the effect of the bending stress on the steel wires in this area cannot be neglected, as it is a factor contributing to the failure of long cables/hangers. We further used a salt spray chamber to simulate an acid-rain environment. The results showed the following: (1) corrosion-fatigue damage of the cables/hangers occurs under the combined action of a corrosive environment and an alternating stress. This leads to an intensified corrosion damage, reduced ductility, increased brittleness, and eventually, brittle fracturing of the cables/hangers. (2) In the same corrosive environment, the highest degree of specimen corrosion occurred during alternating stress, followed by static stress, and no stress. (3) After corrosion-fatigue damage occurred for a specimen, its breaking stress was about 60% in comparison to the uncorroded specimen. The percentage elongation at the break also decreased; this was about 40% in comparison to the uncorroded specimen, indicating brittle fracturing. (4) The steel wires of the cables/hangers with corrosion-fatigue damage are more prone to brittle fracture if they are exposed to complex spatial stresses.

1. Introduction

In recent years, there have been many bridge collapse incidents due to cable/hanger failure (cables of suspension bridges, cables of cable-stayed bridges, or hangers of half-through or through-arch bridges). For example, some of the short hangers of the Xiaonanmen bridge in Sichuan broke on both sides of the deck at 5 : 00 a.m. on November 7, 2001, as shown in Figure 1(a). Similarly, some of the secondary short hangers of the Korla Peacock River bridge in Xinjiang failed at 5 : 00 a.m. on April 12, 2011, as shown in Figure 1(b). In another example, the deck connecting the east and west piers of the 164 meter tied-arch Tongyu River bridge in Binhai County, Jiangsu, collapsed in the early morning of July 11, 2011. Shortly after 8 : 00 a.m. on July 14, 2011, the Wuyishan Gongguan bridge in Fujian collapsed for the second time [2], as shown in Figure 1(c). Finally, the seventh cable/hanger at the north end of the Jinsha River Luoguo bridge in Panzhihua, Sichuan, failed at 6 : 15 a.m. on December 1, 2012 [3], as shown in Figure 1(d).

On August 15, 2018, Italy's Ponte Morandi bridge collapsed (as shown in Figure 1(e)), and it was reported that the steel cable on one end of the column was the first to break at the junction of the steel cable and the bridge [4]. At 9 : 30 a.m. on October 1, 2019, as shown in Figure 1(f), the South Australia sea crossing bridge in Taiwan Province collapsed [5], owing to a steel cable fracture. There are increasingly more cases worldwide where cables/hangers are being

Figure 1: Cable breaking cases of cable bridges [1]: (a) Yibin little south gate bridge; (b) Peacock river bridge, Xinjiang; (c) Wuyishan mansion bridge, Fujian; (d) Sichuan Jinsha River Luoguo bridge; (e) Ponte Morandi bridge, Italy; (f) South Australia sea crossing bridge in Taiwan Province.

replaced in advance owing to the deterioration and damage of the sheath, the corrosion and breakage of wires of the cable body, and other structural damages (e.g., Humen bridge, Jiangyin Yangtze River bridge, Lulin bridge in New Orleans, Maracaibo bridge in Venezuela, Pasco Kennewick bridge in the United States, Wye steel cable-stayed bridge in the United Kingdom, and Köhlbrand Estuary bridge in Germany).

Scholars and experts have conducted much research on the causes of cable/hanger failure and produced valuable results. These results mainly focus on the problems related to short hangers and bridge fatigue and overloading. Liu et al. [6] examined cable/hanger failure with the finite element method and concluded that the second shortest set of hangers is most likely to fail; hence, special attention should be paid to their design and maintenance. Gu et al. [7] developed several solutions after analyzing the mechanical behavior and failure mechanism of the short hangers of half-through and through-arch bridges. They stated that short hangers are under extremely unfavorable conditions when under the action of static and dynamic forces. Chen [8] studied the spatial distribution of forces and the damage mechanism of the short hangers of tied-arch bridges and analyzed the forces acting on these hangers and the factors that make them prone to damage. Liu et al. [9–13] and Guo et al. [13] conducted fretting fatigue tests of bridge cables, examined the corrosion fatigue and electrochemical behavior of steel wire, carried out fatigue evaluation, and studied the reliability of metal. Correia et al. [14] proposed fatigue crack growth modeling for variable amplitude loading.

Previous research focused on analyzing the forces on short hangers or the second shortest set of hangers. The results suggested that short hanger failure is caused by complex stress conditions. The analysis of cable/hanger failure and damage incidents also suggests that failure generally occurs near the top surface of the cross beam above the lower anchorage area. Failure incidents generally occur during off-peak loading. This indicates that cable/hanger failure does not occur during the most unfavorable loading conditions; therefore, this cannot be attributed solely to the stress conditions in or the overloading of the cables/hangers. In the case of Sichuan's Jiangsha River Luoguo bridge, the long cables/hangers in the midspan area of the bridge failed. This shows that the stress conditions of short cables/hangers were not the principal cause of the cable/hanger damage. However, more research is required to investigate whether the Luoguo bridge long cable/hanger failure was an isolated

incident. Therefore, it is necessary to conduct a comprehensive study of the damage and failure mechanisms of cables/hangers by combining experimental simulations with finite element analysis to analyze the corrosion characteristics of the cables/hangers.

2. Spatial Distribution of Forces Acting on Bridge Cables/Hangers

2.1. Bending Stress of the Anchorage Zone. Wu et al. [15] calculated the in-plane eigenfrequencies and vibration mode of horizontal and inclined cables, while considering bending stiffness. They proposed an equation for the bending resistance coefficient $\delta = (\mathrm{EI}/l^3)/(\mathrm{EA}/l) = (\mathrm{EI}/l^2)/\mathrm{EA}$, where δ is the ratio between the bending stiffness of unit volume cable, EI/l^3, and the axial rigidity of unit length cable, EA/l. When the bending resistance coefficient is $\delta < 1 \times 10^{-6}$, the bending stiffness has a very small effect on the eigenfrequency of the cable, and its effect on the cable can thus be ignored. When the bending resistance coefficient, δ, is greater than 1×10^{-6}, the bending stiffness has an increased effect on the natural frequencies of each order. Therefore, its effect on the cable should not be neglected. Thus, the bending resistance coefficient can be used to determine the length of the cable/hanger when it is necessary to consider the effect of the bending stress on the cable/hanger. For example, if a PES (7 mm diameter)-139 cable/hanger with a design force of 357 kN, an outer diameter of 111 mm, and $\delta = 1 \times 10^{-6}$ is considered, the critical length is $l = 27$ m. This indicates that when a cable/hanger exceeds 27 m, the effect of the bending moment can be ignored. In contrast, when a cable/hanger is shorter than 27 m, the effect of the bending moment should be considered. Most cables/hangers that are used near the midspan areas of arch bridges are about 25–30 m long. As a result, it is necessary to consider the effect of the bending stress [16, 17].

Assume that, under the action of a dead load or other external load, there is a deflection, $\Delta\varphi$, between the cable/hanger and the supporting structure (as shown in Figure 2).

Then, for a point on the cable/hanger free-body diagram, the equilibrium equation is as follows:

$$-\mathrm{EI}\frac{d^4x}{dy^4} + \frac{d^2x}{dy^2}\cdot\frac{dy}{ds}N + g_x = 0. \tag{1}$$

It is assumed that the $\Delta\varphi$ deflection of the tension cable/hanger is very small, and the vertical span ratio is very small, so $dy/ds \approx 1$. The equation is solved to obtain the shape function of the cable/hanger:

$$x = a_1 sh(ky) + a_2 ch(ky) + \frac{g_x y(L-y)}{2N} + a_3, \tag{2}$$

where $k^2 = N/\mathrm{EI}$, dx/dy is the sine of the angle between the tangent and the horizontal line at the inspection point of the cable/hanger, g_x is the horizontal component of gravity of a unit length of cable/hanger (constant), N is the vertical component of the cable/hanger tension (constant), M is the bending moment caused by the rotation of the cable/hanger,

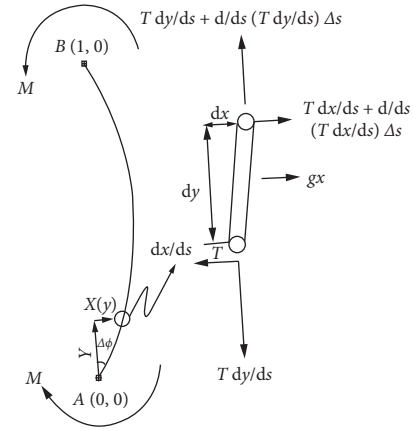

Figure 2: Schematic of cable/hanger forces.

and q is the bending force generated by the rotation of the cable/hanger.

Taking the derivative of the shape equation gives the bending moment equation:

$$\begin{aligned} M(y) &= -\frac{d^2x}{dy^2}\mathrm{EI} = -\left[k^2 a_1 sh(ky) + k^2 a_2 ch(ky) - \frac{g_x}{N}\right]\mathrm{EI} \\ &= -\left\{k^2 a_1\left[sh(ky) - \frac{ch(ky)}{\beta}\right] - \frac{g_x}{N}\right\}\mathrm{EI}, \\ \beta &= -\frac{a_1}{a_2}\ \text{(undetermined constant)}. \end{aligned} \tag{3}$$

During projects where bridge cables/hangers are subjected to full loading, there is a large frictional stress at the joints owing to the confining action of the beam. Therefore, calculations should be carried out under the assumption that these adjacent structures are consolidated. The boundary conditions are as follows:

When $y = 0$ and $x = 0$, $dx/dy = \Delta\varphi$; when $y = 1/2$, $dx/dy = \Delta\varphi = 0$.

Under the action of the axial tensile force, the weight of the cable/hanger is neglected, and the boundary conditions are substituted into equation (4).

In practical engineering, the tension cable/hanger is usually in the state of load holding, N is large, and g_x the horizontal component of the gravity of the tension cable/hanger at the analysis point is small, so the influence of the self-weight of the tension cable/hanger can be ignored, that is, $g_x/N \cong 0$.

When $k^2 = N/\mathrm{EI}$,

$$M(y) = -kEI\left(\Delta\varphi - \frac{g_x l}{2N}\right)e^{-ky} \approx -\sqrt{EIN}\Delta\varphi e^{-ky}. \tag{4}$$

It is evident that the bending moment at each point on the cable/hanger decreases exponentially as the distance y increases. In addition, the maximum bending moment is generated at the anchor point A(0, 0). This also explains why the

cable/hanger damage generally occurs near the top surface of the cross beam above the lower anchorage area. At this time,

$$M_A = -\sqrt{EIN}\Delta\varphi. \quad (5)$$

The bending stress at the anchor point of the cable/hanger can be obtained from

$$\sigma_A = \frac{M_A D}{2I}, \quad (6)$$

where D is the outside diameter of the cable/hanger. The maximum bending stress at the anchorage point due to the deflection of $\Delta\varphi$ owing to dead load or another external load is obtained as follows:

$$\sigma_A = -\frac{D}{2}\sqrt{\frac{\mathrm{EN}}{I}}\Delta\varphi. \quad (7)$$

2.2. Displacement and Deformation of the Anchorage Zone. A half-through-arch bridge with a rigid frame and a span of 160 m, located in Southwest China, was selected for analysis. The bridge has a total of 26 cables/hangers that consist of steel strands. Bridge construction was completed in April 1995; in 2003, all of the cables/hangers were replaced. On December 1, 2012, one of the midspan cables/hangers broke. Because the analysis of cable/hanger failure shows that most incidents occur when a bridge is not under maximum loading, the present finite element model only simulates the spatial stress distribution of cables/hangers under dead load conditions (Figure 3).

During a dead load, both the upper and lower anchorage areas of the cables/hangers undergo displacement and deformation. Because the point where the force is applied is far from the upper anchorage area, its effect on the upper anchorage area is negligible. Consequently, this study only considers the lower anchorage area (Table 1).

Owing to space limitations, only half of the cables/hangers are listed.

It is evident from Figure 4 that, under a dead load, the lower anchorage area of the cable/hanger has undergone displacement and rotation. The displacement along and transverse to the bridge axis was small. Most of the displacement occurred along the vertical direction; the maximum displacement was around 40 mm. In terms of the rotation angle, the change in the rotation angles of the lower anchorage zone was symmetrical in the transverse direction. The largest rotation angles occurred at the ends of the bridge, and smaller rotation angles occurred along the span. Along the axial direction, with the exception of the short cables/hangers at both ends of the bridge where the rotation angles were relatively small, a large rotation occurred for the remaining cables/hangers. This is consistent with existing research on the structural behavior of short cables/hangers. Assuming a PES 7 mm diameter-139 cable/hanger with an outer diameter of 111 mm, $E = 1.95 \times 10^5$ MPa, $I = A(D^2/16)$ under a dead load, and a rotational angle of 0.00113 rad, and the bending stress is as follows:

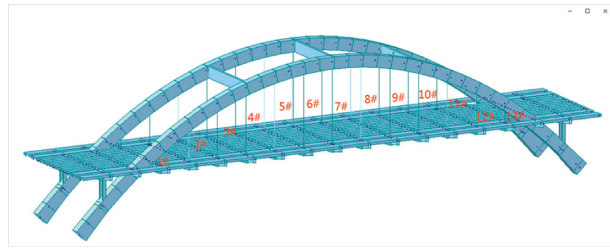

Figure 3: A bridge in Southwest China.

$$\sigma_A = -\frac{D}{2}\sqrt{\frac{\mathrm{EH}}{I}}\Delta\varphi = 18.8\,\mathrm{MPa}. \quad (8)$$

Under a dead load, the rotation angle of the lower anchorage zone is 0.00113 rad and the bending stress generated at this point is 18.8 MPa. Because of construction deviations, fatigue loading or overloading would cause this angle to increase. Especially in the case of half-through and through steel arch bridges without constraining ties, the cables/hangers are anchored directly to cross beams. Under the action of horizontal forces, the cross beam undergoes a horizontal displacement. As a result, bending occurs in the lower anchorage area of the cables/hangers. This causes the bending stress at the end of a cable/hanger to increase.

3. Corrosion-Fatigue Damage Mechanism of Arch Bridge Cables/Hangers under the Combined Effect of Alternating Load and Environment

Case studies show that cable/hanger failure generally occurs near the lower anchorage area. Although the cable/hanger sheath in the lower anchorage area was not cracked, some deterioration and damage were present. This allowed rainwater to seep through the sheath and come into contact with the steel cable. After cutting the PE (polyethylene) sheath, the collected water caused severe corrosion of the steel wires in the lower anchorage area (Figure 5). Further investigations revealed that these service cables/hangers had been subjected to continuous action of alternating loads (including dead load, vehicle load, and wind load). The research on the corrosion of stay cables at home and abroad is limited to the material corrosion under the nonstress state and the stress corrosion under static load. The research on the fatigue of stay cables is limited to the effect of fatigue load without considering the coupling effect of environmental corrosion. Therefore, a corrosion-fatigue test of the steel wires under the combined effects of a corrosive environment and an alternating load was required for further understanding the failure mechanism of the cables/hangers.

3.1. Corrosion-Fatigue Testing of the Cables/Hangers. The test material was a galvanized steel wire with a diameter of 7 mm and a tensile strength of 1860 MPa. The weight of the galvanized layer of a single steel strand was ≥110 g/m^2. Each strand had a length of 5.4 m, and three sets of wires were used for each working condition. The test was carried out

Table 1: Displacement and rotation of upper and lower cable/hanger anchorage areas under dead load.

Number	Cable length (m)	dx (mm)	dy (mm)	dz (mm)	rx (rad)	ry (rad)	rz (rad)
#1	5.588	−0.4120	0.7651	−8.7577	−0.00097	0.001207	0.000038
#2	9.58	−0.4815	0.9024	−16.3449	−0.00113	0.001136	0.000024
#3	12.772	−0.5465	0.9209	−23.6885	−0.00115	0.001071	0.000009
#4	15.21	−0.5707	0.9119	−30.3341	−0.00114	0.000914	0.000008
#5	16.945	−0.5465	0.9085	−35.5876	−0.00114	0.000660	0.000010
#6	17.959	−0.4802	0.9079	−38.9308	−0.00113	0.000340	0.000011
#7	18.314	−0.3747	0.9073	−39.9846	−0.00113	−0.000027	0.000011
#8	17.959	−0.2459	0.9079	−38.5742	−0.00113	−0.000389	0.000012
#9	16.945	−0.1137	0.9086	−34.9270	−0.00114	−0.000697	0.000013
#10	15.21	0.0115	0.9121	−29.4689	−0.00114	−0.000933	0.000014
#11	12.772	0.1134	0.9215	−22.7524	−0.00115	−0.001069	0.000014
#12	9.58	0.1874	0.9030	−15.4820	−0.00113	−0.001112	−0.000002
#13	5.588	0.2600	0.7602	−8.1027	−0.00097	−0.001162	−0.000021

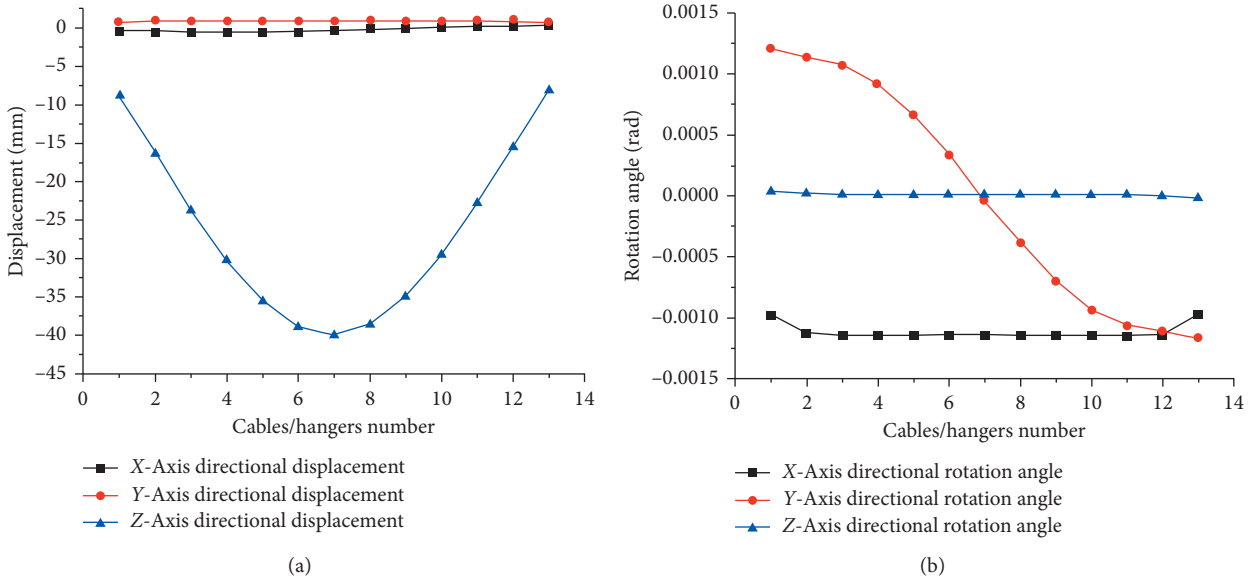

(a) (b)

Figure 4: Displacement and angle curve of lower anchorage zone: (a) displacement curve of the lower anchorage zone; (b) R-angle curve of the lower anchorage zone.

(a) (b)

Figure 5: Serious corrosion of steel wires in the lower anchorage area.

based on the China standard (2013), "Corrosion tests in artificial atmospheres—Salt spray tests." The acid-rain environment was simulated in a salt spray chamber based on the average ion concentration of acid rain in Southwest China over the past five years. An accelerated corrosion test was used to simulate the corrosion of the samples in acid rain under three different working conditions: no load, static load, and an alternating load. To accelerate the corrosion of the samples, the simulated acid-rain concentration was significantly higher than the ion concentration of the acid rain in Southwest China.

According to the people's Communications Press (2007), "Guidelines for Design of Highway Cable-stayed Bridges," for a galvanized steel wire with a tensile strength of 1860 MPa, the allowable stress is 744 MPa. A calibrated self-locking hydraulic jack was used to apply an alternating stress; the upper limit was 744 MPa, and the lower limit was 544 MPa. The upper and lower limits were applied alternatively every 2 h; the test was carried out without interruptions. The test time for each working condition was 120 h, 360 h, and 720 h. The samples, which were corroded under different working conditions, were subjected to a tensile test using a universal tester to obtain the post-corrosion mechanical properties of the samples. The obtained results were compared with the mechanical properties of the uncorroded specimens [18, 19].

3.2. Corrosion-Fatigue Damage Mechanism of Cables/Hangers. The tensile fracture analysis of the specimens under each working condition yielded the following results. The uncorroded steel wire specimen exhibited a cup-and-cone fracture type, as shown in Figure 6. In a corrosive environment, the no-stress specimens also exhibited a cup-and-cone fracture type, as shown in Figure 7(a). Most of the static-stress specimens displayed a milling-cutter-type fracture, as illustrated in Figure 7(b). A few samples exhibited a cup-and-cone fracture type; most of the alternating stress specimens featured a cleavage-milling-cutter fracture type, as presented in Figure 7(c). A few specimens also exhibited a milling-cutter fracture type and a combination of other fracture types; the cleavage fracture type is presented in Figure 7(d). Macroscopic images of typical fractures are shown in Figure 7.

In Figure 7, necking of the wire can be observed in the specimens with the cup-and-cone and the milling-cutter fractures; the former has more deformation. Necking is a form of plastic deformation associated with ductile materials. This means that cup-and-cone and milling-cutter fractures are ductile fractures. In Figures 7(c) and 7(d), no necking occurred near the cleavage and the cleavage-milling-cutter specimens. This is due to their reduced ductility and increased brittleness. These fractures can be classified as brittle-type fractures.

The above analysis of fracture types indicates that the uncorroded steel wire exhibited ductile fracturing and obvious necking. The corroded specimens subjected to no-stress and static-stress conditions in an acid-rain environment displayed ductile and brittle fracturing. Further corroded specimens were subjected to an alternating stress and a corrosive environment. The ductility of the specimens decreased, while their brittleness increased as corrosion progressed with time. This ultimately resulted in brittle-type fracturing [1], and local corrosion and corrosion histograms of steel strands under different stress loadings are shown in Figure 8.

3.3. Corrosion-Fatigue Performance of Cables/Hangers. The corrosion-time and tensile-strength relationship curves show that early-stage corrosion (i.e., corrosion only on the specimen surface), has a small effect on the mechanical properties of the cable/hanger. On the contrary, after 360 h of corrosion and under alternating stress, the breaking stress of the specimens decreased significantly. The breaking stress of one specimen decreased to only about 1300 MPa (Figure 9); this resulted in its sudden fracturing. In this case, the combined effect of an alternating stress and a corrosive environment resulted in corrosion-fatigue damage of the steel wire [20, 21]. As a result of the cyclic action of alternating stress, a slip zone formed on the surface of the specimen. The formation of the slip zone was accelerated by the corrosive environment. As time progressed, some microcracking was observed on the specimen surface. This suggests that the internal crystal structure of the specimen had changed, resulting in reduced ductility and increased brittleness of the specimen and its subsequent fracturing. The percent elongation at the break reflects the plastic deformation capacity of the material at the time of fracture. Figure 9 shows that, as time progresses, the percent elongation at the break of the corroded specimens under all three working conditions displays a decreasing trend. The percent elongation at the break was lowest under alternating-stress conditions, with a minimum value around 3%. This was followed by the elongation under static-stress conditions. As a comparison, the percent elongation at the break decreased by only about 40% for the uncorroded specimens. A few alternating stress specimens exhibited brittle fracturing; their breaking stress equivalent was only about 60% of the uncorroded specimens. Under the no-load conditions, the percent elongation at break was affected but not significantly [22, 23].

When considering the mechanical properties of short and long cables/hangers, factors inducing cable damage, such as bending stress and fatigue loading, can be addressed through engineering and technology. For example, this can be accomplished by increasing the safety factor or by using high-strength stainless steel wires (the Research Institute of Highway Ministry of Transport is conducting research on high-strength stainless steel wires [24]). However, once the outer sheath breaks, rainwater can penetrate through the surface cracks and comes into contact with the cable strands. As the cable vibrates, the water flows down and collects in the lower anchorage area. This creates an environment that combines acid-rain-induced corrosion with alternating load conditions [25, 26]. As a result, the steel wires in this area are subjected to corrosion-fatigue damage and their ductility

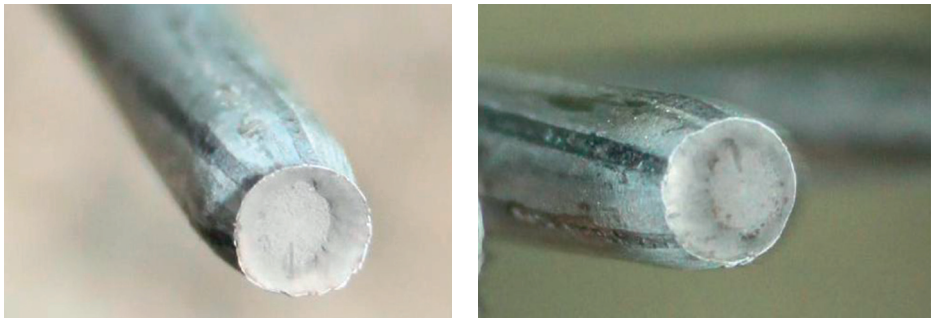

(a) (b)

Figure 6: Fracture of uncorroded steel strand wire.

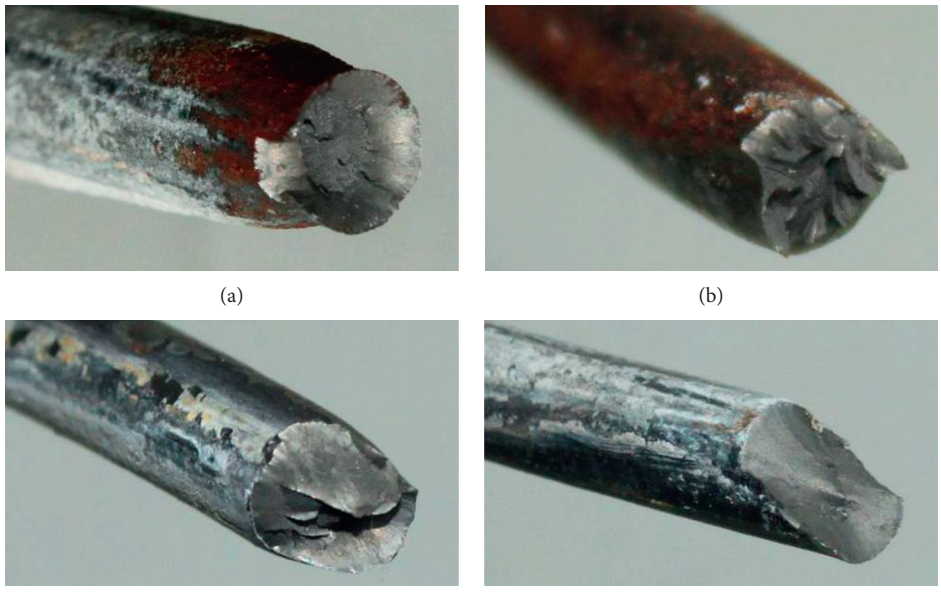

(a) (b)

(c) (d)

Figure 7: Fracture types of corroded steel strand wires: (a) cup-and-cone fracture; (b) milling-cutter fracture; (c) cleavage-milling-cutter fracture; (d) cleavage fracture.

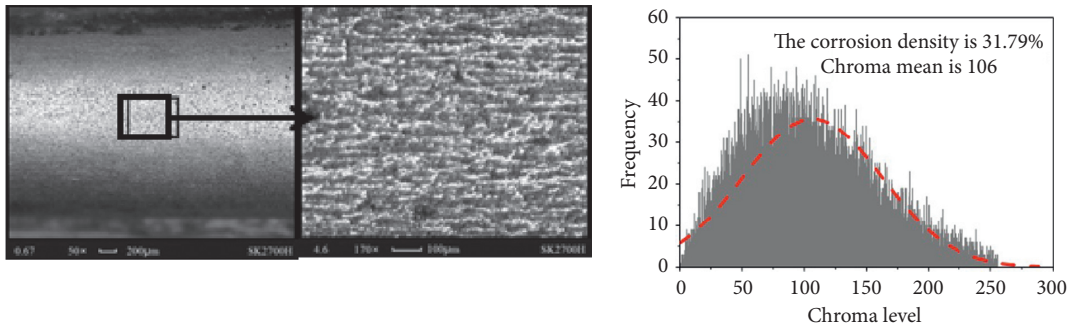

(a) (b)

Figure 8: Continued.

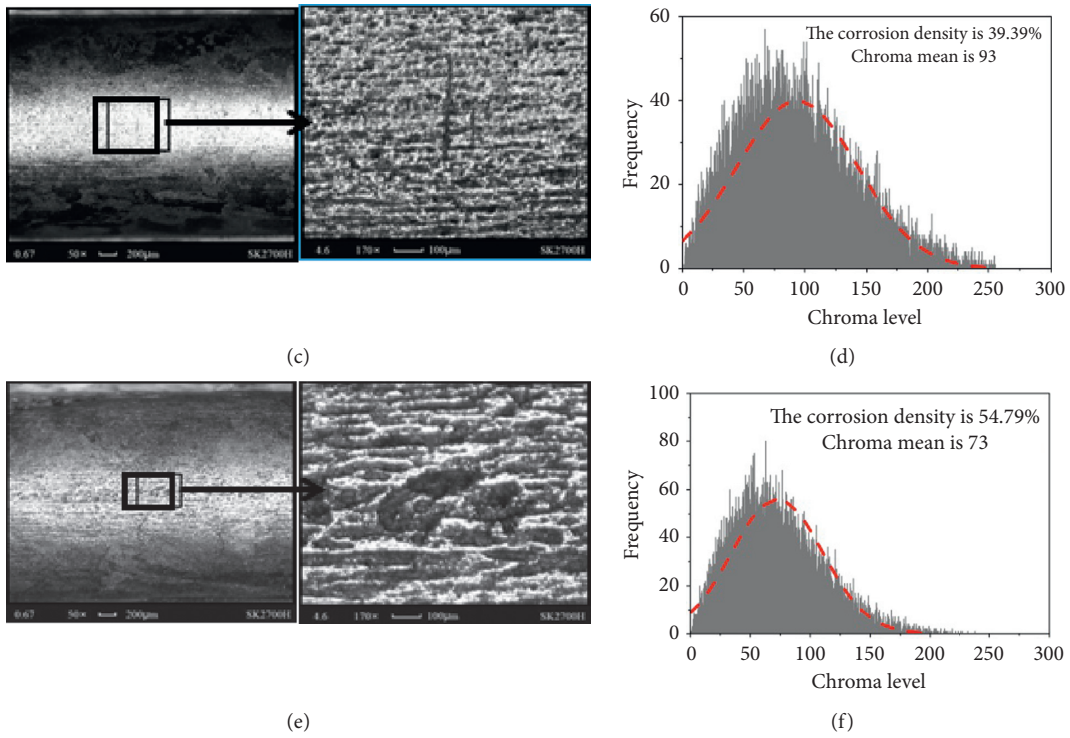

Figure 8: Local corrosion and corrosion histogram of steel strand under different stress loadings: (a) local corrosion figure under no stress (720 h); (b) corrosion histogram of no stress; (c) local corrosion figure under static stress (720 h); (d) corrosion histogram of static stress; (e) local corrosion figure under alternating stress (720 h); (f) corrosion histogram of alternating stress.

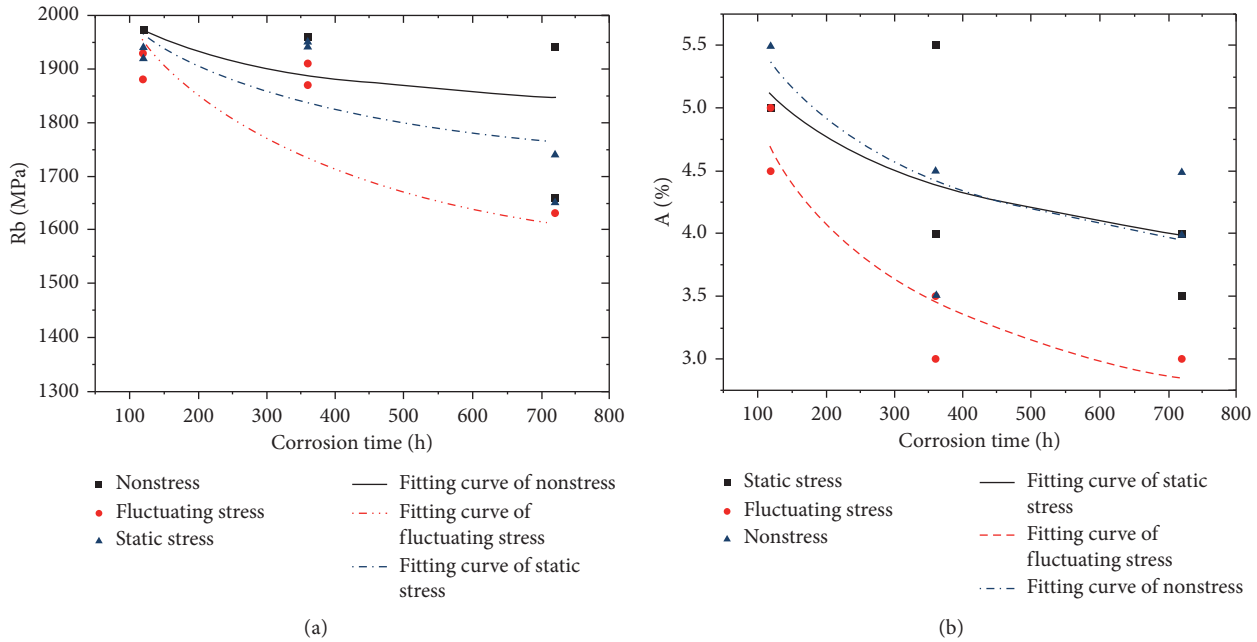

Figure 9: Mechanical parameters under different loading conditions [19]: (a) breaking strength Rb; (b) elongation A (%).

decreases, while their brittleness increases. Finally, after the added action of complex spatial stresses, the cable/hanger becomes prone to failure.

4. Conclusions

The main conclusions are the following: (a) bending stress is one of the factors that causes damage to long cables/hangers. It is necessary to improve the quality control measures during construction. In addition, there needs to be a reduction in the errors during the installation of cable anchorages. There also needs to be a limit for the occurrence of bending stress, while increasing the safety factor of cables/hangers. (b) In a corrosive environment, the degree of specimen corrosion varies under different load conditions. When corrosion occurred, the specimens under alternating stress exhibited the highest degree of corrosion, followed by the static-stress specimens, and finally, the no-stress specimens. After 720 h of corrosion, the percent elongation at the break of the specimens under an alternating stress decreased significantly; this was around 40% in comparison to the uncorroded specimens. Moreover, the breaking stress of the alternating stress specimens was only 60% in comparison to the uncorroded specimens; this indicates a brittle fracture type. (c) The corrosion-fatigue damage of steel wire cables/hangers resulted in reduced ductility and increased brittleness of the steel wire. By adding complex spatial stresses on the short and long cables/hangers, the risk of sudden cable/hanger failure increases significantly.

Data Availability

The data used to support the findings of this study are available from the corresponding author upon request.

Conflicts of Interest

The authors declare that they have no conflicts of interest.

Acknowledgments

This paper was supported by the Program of the National Key R&D Plan of China (Grant no. 2017YFC0806001) (Overload monitoring and early warning system and security risk control technology for the urban expressway bridge) and the Major National Natural Science Foundation for Research Instrument Development of China (Grant no. 11627802) (Development of a structural fatigue testing system under complex environment).

References

[1] S. C. Yang, J. Q. Zhang, and G. W. Yao, "Mesoscopic damage behavior of corroded steel strands based on image grayscale analysis," *Journal of Solid Mechanics*, vol. 39, no. 3, pp. 284–294, 2018.

[2] J. X. Wu and E. D. Liu, "Bridge hanger breakage causes and early warning technology," *Western Transportation Science and Technology*, vol. 34, pp. 51–55, 2013.

[3] Z. Ma, "Sichuan panzhihua jinsha river bridge with slings broken deck collapse," 2012.

[4] X. Nan, S. Xiao, and C. Co, "The collapse of italian bridge exposed the weakness of reinforced concrete," *Hidden Dangers of Multinational Bridges*, vol. 34, 2018.

[5] H. Guo, "12 people injured and 5 people missing in the collapse of south australia sea crossing bridge in yilan," 2019.

[6] E. D. Liu, G. M. Liao, and G. D. Tang, "Analysis on the rupture of the drawers of Arch Bridge," *Northern Transportation*, vol. 11, pp. 61–63, 2013.

[7] A. B. Gu and J. L. Xu, "Analysis of the structural behavior of the through arch bridge with short tension slings," *Journal of Chongqing Jiaotong University*, vol. 21, no. 4, pp. 1–3, 2002.

[8] J. Q. Chen, *Study on Spatial Stress Characteristics and Damage Mechanism of Short Tension Cable of Tied Arch Bridge*, Chongqing Jiaotong University, Chongqing, China, 2013.

[9] Z. Liu, M. H. Hebdon, A. José, and F. O. Correia, "Fatigue assessment of critical connections in a historic eyebar suspension bridge," *Journal of Performance of Constructed Facilities*, vol. 34, 2019.

[10] Z. Liu, J. Correia, H. Carvalho et al., "Global-local fatigue assessment of an ancient riveted metallic bridge based on submodelling of the critical detail," *Fatigue and Fracture of Engineering Materials and Structures*, vol. 34, 2019.

[11] Z. Liu, T. Guo, J. Correia et al., "Reliability-based maintenance strategy for gusset plate connections in steel bridges based on life-cost optimization," *Journal of Performance of Constructed Facilities*, vol. 34, 2020.

[12] Z. Liu, T. Guo, X. Yu et al., "Corrosion fatigue and electrochemical behaviour of steel wires used in bridge cables," *Fatigue & Fracture of Engineering Materials & Structures*, vol. 34, 2020.

[13] T. Guo, Z. Liu, J. Correia et al., "Experimental study on fretting-fatigue of bridge cable wires," *International Journal of Fatigue*, vol. 34, 2020.

[14] J. Correia, H. Carvalho, G. Lesiuk et al., "Fatigue crack growth modelling of Fão Bridge puddle iron under variable amplitude loading," *International Journal of Fatigue*, vol. 34, 2020.

[15] Q. X. Wu, L. Li, and B. C. Chen, "A theoretical formula for calculating the in-plane natural vibration of a tension sling considering bending stiffness," *Engineering Mechanics*, vol. 27, no. 11, pp. 9–15, 2010.

[16] X. F. He and A. R. Chen, "Analysis of local bending stress of cable-stayed slings for cable-stayed bridges," *Shanghai Highway*, vol. 90, 1999.

[17] W. S. Zheng, "Discussion on bending stress and control countermeasures of cable-stayed bridge slings," *Highway Traffic Technology*, vol. 23, no. 5, pp. 90–93, 2013.

[18] W. Z. Li, *Experimental Study on Stress Corrosion and Corrosion Fatigue of Stay Cables under Salt spray*, Chongqing Jiaotong University, Chongqing, China, 2015.

[19] G. W. Yao, C. Y. Liu, and G. Q. Wu, "Acid rain environment-load coupling effect of load coupling on corrosion damage mechanism of pull sling," *Journal of Chongqing Jiaotong University (NATURAL SCIENCE EDITION)*, vol. 12, no. 6, pp. 6–10, 2016.

[20] D. G. Harlow, "Probability approach for prediction of corrosion and corrosion fatigue life," *AIAA Journal*, vol. 32, no. 10, pp. 2073–2079, 2004.

[21] S. C. Yang, G. W. Yao, and J. Q. Zhang, "Observations on the damage behaviors of corrosion fatigue in steel strands based on image analysis," *Advances in Mechanical Engineering*, vol. 9, no. 12, pp. 1–10, 2017.

[22] Y. Xu, *Study on Degradation of High Strength Cable Steel Wire in Corrosive Environment*, University of Technology, Harbin, China, 2014.
[23] K. Suzumura and S. Nakamura, "Environmental factors affecting corrosion of galvanized steel wires," *Journal of Materials in Civil Engineering*, vol. 6, p. 67, 2012.
[24] C. C. Li, J. Q. Zhang, H. M. Wang, J. C. Cao, and J. W. Zhang, "Experimental study on high strength stainless steel wire," *Highway Traffic Technology*, vol. 23, no. 8, pp. 102–107, 2013.
[25] J. Toribio, B. González, and J.-C. Matos, "Analysis of fatigue crack paths in cold drawn pearlitic steel," *Materials*, vol. 8, no. 11, pp. 7439–7446, 2015.
[26] A. Laurino, E. Andrieu, J.-P. Harouard, G. Odemer, J.-C. Salabura, and C. Blanc, "Effect of corrosion on the fatigue life and fracture mechanisms of 6101 aluminum alloy wires for car manufacturing applications," *Materials & Design*, vol. 53, p. 236, 2014.